JOURNAL OF CATALYSIS 104, 120–135 (1987)

Oxygen Vacancy Model in Strong Metal–Support Interaction

M. G. SANCHEZ AND J. L. GAZQUEZ[1]

W. R. Grace & Company, Technical Group, 7379 Route 32, Columbia, Maryland 21044

Received December 9, 1985; revised October 7, 1986

A model is proposed to account generically for strong metal–support interactions, a term which is used in a broad sense, and for SMSI, an acronym which is used in a specific and narrow sense. The generalized model is operative through the interaction of metal atoms with oxygen ion lattice vacancies in oxide supports. The occupancy of vacancies by metal atoms is equally applicable to different oxide systems, but the resulting effects may vary profoundly depending on the nature of the support. When applied to fluorite-type oxide supports, the model accounts for experimental observations of high metal dispersion, high sorption, and high catalytic activity, and unusual stability of these against sintering, up to temperatures ca. 1400 K under strong oxidation conditions. In contrast, when applied to rutile the model accounts for SMSI. The marked differences in behavior of metals on the two types of supports is explained on the basis of the uniformly compact or localized open cation sublattices. On the first type, interactions are mainly limited to metal occupancy of surface vacancies due to the diffusion barrier created by the support cations. In the second type, metal diffusion into support bulk vacancies and metal burial are possible, under hydrogen reduction, because of the open nature of the cation sublattice. The opposite phenomenon, dislodging the metal back to the support surface through oxidation, is also presented. As such, the model accounts for the typical observations in SMSI systems. The model has predictive value.

INTRODUCTION

General Background

The interaction between metal and support in supported metal catalysts has been of scientific and industrial interest for many years. Electronic interactions between Group VIII metals and semiconductors have been studied for over 40 years. In the last 20 years, the development of automobile exhaust catalysts led to intensive investigations of noble metals and their interactions with supports such as transition aluminas and other oxides. In particular, Sanchez *et al.* (*1*) and Sergeys *et al.* (*2*) studied oxide supports which exhibit the fluorite structure.

More recently, Tauster and co-workers (*3*, *4*) discovered unusual effects in a series of metal/oxide support systems. They introduced the acronym SMSI to refer to a strong metal–support interaction that was observed. Their pioneering work has resulted in much activity in this area in the last 7 years. The original observations have been amply confirmed and new systems have been shown to exhibit equivalent behavior.

At the outset, it should be stated that the expression "strong metal–support interaction" will be used in this paper in a generic sense, while the acronym SMSI will be reserved for those cases which meet the specific and narrow meaning in the original work, and equivalent subsequent research. The two expressions should not be confused.

In order to avoid misunderstandings we shall call SMSI any metal–support interaction which meets the criteria explicitly or implicitly set by the original authors (*3–6*) in 1978–1979 which are the following:

(a) Initial high metal dispersion after low temperature reduction (LTR), which results in

[1] Present address: Departamento de Química, Universidad Autónoma Metropolitana, Iztapalapa, Mexico D.F. 09340, Mexico.

0021-9517/87 $3.00

small crystallite size
high sorption
high relative catalytic activity, and
"normal" crystallite morphology.

(b) After high-temperature hydrogen reduction (HTR) in the range of about 700–1100 K, the system exhibits
a sharp decrease in sorptive properties,
a sharp decrease in relative catalytic activity for many hydrocarbon conversion reactions,
an increase in metal particle cross sec- "flat," thin, polygonal, metal shape (pill-box), and
reduction of some of the support cations.

(c) Virtual return to condition (a), except in size, after high-temperature oxidation (HTO) with H_2O or O_2 and LTR in H_2.

Thus, (*1*) and (*2*) observed metal–support interactions which gave high metal dispersion and resulted in high sorption, good catalytic activity, and high thermal stability, under oxidation conditions, up to temperatures ca. 1400 K, in oxide supports possessing the fluorite structure. In contrast, other authors (*3–6*) observed SMSI in TiO_2 and other reducible oxides.

While facts relating to SMSI are solidly established, their explanation has been elusive. Several mechanisms and models have been proposed but, as yet, none has been widely accepted. However, two models have received the most attention.

Initially, electronic effects were invoked to rationalize the SMSI. Theoretical calculations by Horsley (*7*) implied that bonding between the metals and the reduced cations in the support could occur and account for the morphological, sorptive, and catalytic changes observed. Spectroscopic data were interpreted as the result of charge transfer to the noble metal. Subsequent research by Huizinga and co-workers (*8–10*) and Short (*11*) has created doubts about this explanation.

More recently, Meriaudeau (*12*), Santos (*13*), Resasco (*14*), and others have invoked support migration to account for SMSI.

The basic idea is that partially reduced oxide support species are able to migrate through or across the metal particles to cover some or most of their surface, thereby blocking sites for sorption and catalysis. This model, while accounting for many observations, is not without controversy. However, in spite of these and other shortcomings, it remains the most widely accepted explanation and rationalization of SMSI to date.

In 1974, (*1*) proposed a tentative model and explanation for metal interactions with ionic oxide supports in general and, more particularly, with those possessing the fluorite structure. The model was limited to surface dispersion of the metal and involved surface oxygen ion vacancies and their occupancy by the metal atoms or "nesting." It could be operative with reducible as well as nonreducible oxide phases.

The purpose of this paper is to propose a model to account for the metal–support interactions observed by (*1*) and (*2*) and for the SMSI observed by (*3*), (*4*), and others. The model, which is an extension of the one suggested by (*1*) in 1974, involves the occupancy of oxygen ion vacancies in the oxide support by metal atoms. While the basic operative mechanism is essentially the same for different systems, its effects and manifestation may vary profoundly depending on the crystal structure of the support.

Only two dioxide structures (fluorite and cassiterite) will be discussed in this paper, although the model should be applicable to any oxide phase which exhibits O^{2-} vacancies. So far, none of the explanations offered for SMSI invokes O^{2-} vacancies as the dominant factor, although some authors make incidental mention of vacancies in their model (*6, 7, 14–17*).

Vacancies will appear, when (a) hydroxylated surfaces are dehydrated, (b) some of the cations in an oxide are reduced by chemical means or by thermal dissociation,

(c) some of the cations of a nonreducible oxide are isomorphously replaced by cations of lower valence, or (d) by combinations of the above.

Unless stated otherwise, interaction and activation energies will be expressed in kcal mol^{-1} (1 kcal = 4.186 kJ) and distances in terms of the oxygen ionic radius of the applicable oxide support. The term "vacancy" (V) will mean the absence of an O^{2-} from the crystal bulk while the term "nest" (N) will mean the absence of O^{2-} or OH^- from the crystal surface. Certain combinations of Vs and Ns will be designated "wells" (W).

The Fluorite Structure

Compounds which are predominantly ionic and contain large cations pack so that the chief contacts are between atoms of opposite sign and so that each atom is surrounded by the maximum number of atoms of the opposite sign (*18*).

Dioxides (MO_2) in which M^{4+} is especially large in relation to O^{2-} are likely to possess the cubic fluorite structure: O_{h-5} (Fm3m) in which M^{4+} is surrounded by eight oxygens and each bulk O^{2-} is surrounded by four M^{4+}. The unit cell edge corresponds to the distance between alternate O^{2-} along the ⟨100⟩ axis. A simple calculation shows that for spherical ions contact between M^{4+} and its eight coordinated O^{2-} will occur only when the radii ratio of M^{4+} to O^{2-} is at least $(\sqrt{3} - 1)$. According to Wyckoff (*18*), "this relation is fulfilled for compounds with the fluorite arrangement."

The presence of vacancies in fluorite-type oxides and the properties which they impart have been known and studied for many years—in particular, their role in diffusion phenomena and on electrical properties (*19–21*). The concentration of vacancies may range up to ca. 17% of the oxygen sublattice without phase transformation and the activation enthalpy for ionic conductivity which depends on O^{2-} diffusion may range between about 15 and 30 kcal mol^{-1} depending on specifics (*19*). The reason for the high activation enthalpy relates to the coordination of the oxygen which is "caged" within four cations. The cation sublattice is uniformly compact and for the ideal structure, the ratio of the opening between adjacent cations to the O^{2-} diameter is $(1 + \sqrt{2} - \sqrt{3})$ or 0.682. As such, the cation sublattice is *always* a barrier, to O^{2-} bulk diffusion in fluorite-type oxides. Table 1 gives dioxides with the fluorite structure showing the O^{2-} and M^{4+} ionic radii according to Wyckoff's guidelines.

Figure 1a is a representation of a cross section of the structure of ThO_2, which is a fluorite-type oxide. It shows a [010] plane of O^{2-} and the corresponding Th^{4+} planes directly in front of and behind it. The [001] surface is fully hydroxylated. Note the tetrahedral coordination of the bulk O^{2-} by Th^{4+} and the resulting cage effect which restricts all oxygens except those on the surface.

Figure 1b is a generalized representation

TABLE 1

Fluorite-Type Metal Oxides

Compound (nominal formula)	Dimensions (Å)[a]		
	Unit cell edge[b]	Cation radius	Oxygen radius
α-PoO_2	5.687	1.041	1.422
ThO_2	5.595[c]	1.024	1.399
PaO_2	5.505	1.007	1.376
PrO_2	5.469	1.001	1.367
UO_2	5.468	1.001	1.367
NpO_2	5.434	0.994	1.359
CeO_2	5.426[c]	0.993	1.356
PuO_2	5.396	0.988	1.349
AmO_2	5.376	0.984	1.344
CmO_2	5.372	0.983	1.343
TbO_2	5.220	0.955	1.305
ZrO_2[d]	5.140[c]	0.941	1.285
HfO_2[d]	5.115	0.936	1.279

[a] 1 Å = 0. 1 nm.

[b] From (*18*) or (c) from (*22*).

[d] Fluorite structure only at high temperature or with stabilizers.

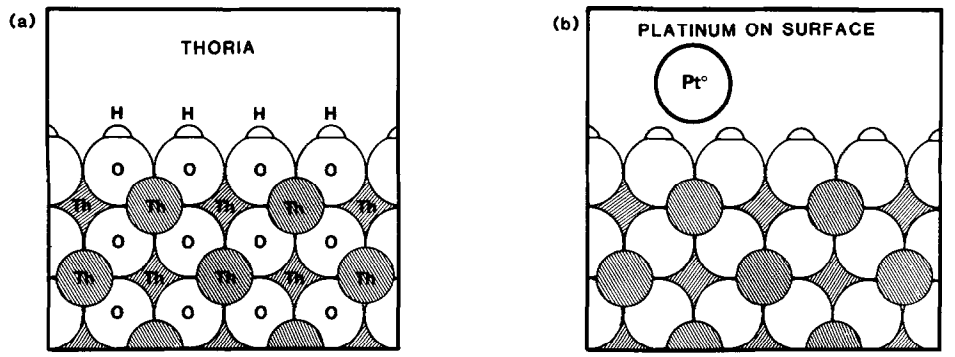

FIG. 1. (a) Cross section of ThO_2 showing a [010] plane of oxygen ions and adjacent thorium cations. The [001] surface is fully hydroxylated. (b) Same as (a) showing a surface platinum atom.

of a fluorite-type oxide support which shows a platinum atom on the [001] surface. Because it does not possess any nests or other imperfections, we refer to it as an ideal surface. The [001] facet has been selected to illustrate a typical hydroxylated fluorite-type oxide because it is easy to visualize, is highly symmetrical, has a high OH^- surface density, and is the crystal form most often found in nature in fluorite oxide minerals, such as thorianite and uraninite (*23*).

The Cassiterite Structure

The most common dioxide structure of metals with octahedral coordination shows tetragonal symmetry, D_{4h-14}(P4/mnm), and is typified by cassiterite (SnO_2) (*18*). It has been selected for our study because TiO_2, the first and most studied SMSI support, exhibits this structure (rutile). Figure 2 shows the rutile unit cell. Figure 3a shows the relative position of the ions in two adjacent layers which are perpendicular to the ⟨001⟩ axis. Any size crystal of rutile may be represented by extension and repetition of these two bulk layers. The corresponding surface layer may be totally or partially hydroxylated. As in fluorite-type oxides, we have chosen to consider a fully hydroxylated surface. One may visualize such a surface as resulting from the hydration of the bulk layers shown in Fig. 3a by adding an OH^- directly above each shaded O^{2-} and one H^+ to each O^{2-} shown in white. In this manner Ti^{4+} is not exposed and becomes octahedrally coordinated with O^{2-}, the surface terminates in OH^-, and the crystal retains electrical neutrality and surface symmetry. Note the two OH^- layers separated by a distance of $c_0/2$.

Tetravalent cations with ionic radii between about 0.5 and 0.75 Å often exhibit octahedral coordination with oxygen and exhibit the cassiterite structure as shown in Table 2 (*18*). The oxygen radii (r_0) are computed from the unit cell edge (a_0) and the octahedral coordination cation radii (r_c), using the relationship

$$r_0 = \frac{\sqrt{2}a_0 - 2r_c}{4} \qquad (1)$$

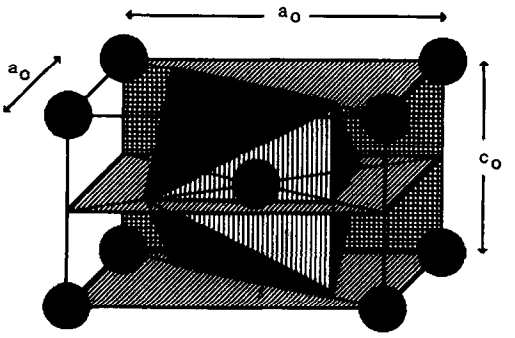

FIG. 2. Tetragonal rutile unit cell. The circles represent Ti^{4+}. The larger O^{2-} (not shown) are centered at the corners of the octahedron.

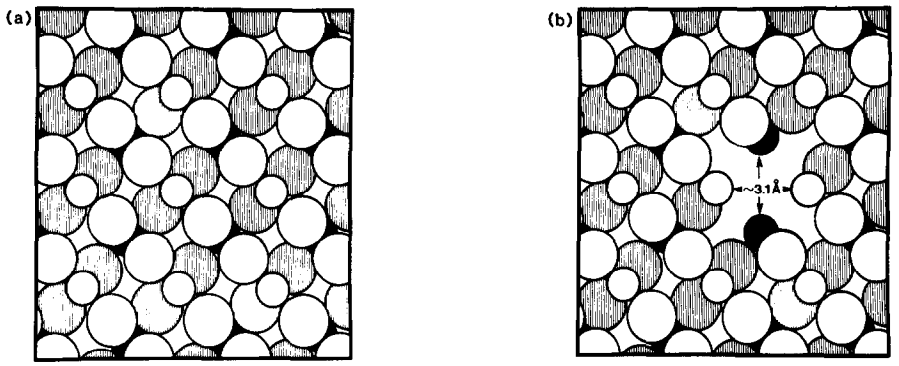

FIG. 3. (a) Relative position of O^{2-} and Ti^{4+} in two adjacent [001] bulk layers of rutile. The small circles represent Ti^{4+} and the large circles represent the O^{2-}. The dark layer is behind the white one at a distance of $c_0/2$. They are identical but at a right angle with respect to each other. Note the O^{2-} which occurs always in pairs. (b) Same as (a) after reduction and selective removal of O^{2-} to form channel. Some of the Ti^{4+} has become Ti^{3+}. The most restrictive dimension within a channel is ~3.1 Å. Note the larger dimensions in other directions. The channel can accommodate large atoms and small molecules.

which has been derived from structural considerations.

In contrast to the fluorite-type oxides, the O^{2-} in cassiterite-type supports is not caged by cations and its diffusion in the presence of O^{2-} vacancies is not blocked by the cation sublattice, at least in the ⟨001⟩ direction. In other ⟨*hkl*⟩ directions, diffusion is hindered to varying degrees. Figure 4 shows four adjacent strands of O^{2-} in rutile which are parallel to the ⟨001⟩ axis and which terminate in OH^-. The Ti^{4+} are not shown. They are located outside of the four strands. Layer 1 contains OH^- but no

TABLE 2

Cassiterite-Type Oxides

Compound (nominal formula)	Dimensions (Å)			
	a_0	c_0	Cation radius[a]	O^{2-} radius
NbO_2	4.77	2.96	0.74	1.32
TaO_2	4.709	3.065	0.73[b]	1.30
SnO_2	4.737	3.186	0.71	1.32
WO_2	4.86	2.77	0.70	1.37
MoO_2	4.86	2.79	0.70	1.37
TeO_2	4.79	3.77	0.70	1.34
TiO_2	4.594	2.958	0.68	1.28
IrO_2	4.49	3.14	0.68	1.25
RuO_2	4.51	3.11	0.67	1.26
VO_2	4.54	2.88	0.63	1.29
β-MnO_2	4.396	2.871	0.60	1.25
CrO_2	4.421	2.926	0.58	1.27
GeO_2	4.395	2.859	0.53	1.29

[a] Octahedral coordination; from (*24*).
[b] Estimated.

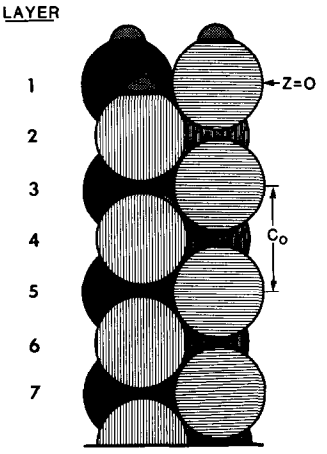

FIG. 4. Detail of oxygen structure in rutile showing four adjacent strands of O^{2-} along the ⟨001⟩ axis which terminate in OH^-. The Ti^{4+} which are located outside of the strands are not shown. Hydration layer 1 contains OH^- but no Ti^{4+}. Layer 2 contains Ti^{4+} and OH^-. Those two layers constitute the [001] hydrated surface. All other layers exhibit O^{2-} and Ti^{4+} in a 2 to 1 ratio. Gradual removal of OH^-, and then O^{2-}, creates large nests and, eventually, wells and diffusion channels.

Ti^{4+}. Layer 2 contains two OH^- ions per Ti^{4+}. Those two layers constitute the [001] hydrated surface. The remaining bulk layers consist of O^{2-} and Ti^{4+} in a 2 to 1 ratio.

In layer 1, a single nest may be formed by the removal of one molecule of water. Two nests may migrate at high temperature to form a pair and several such nests may coalesce into a dehydrated surface region which may appear as a depression. An important point to remember is that in layer 1 removal of OH^- ions can be achieved by dehydration and does not require reduction. In layer 2, the elimination of OH^- ions may result from the reduction of an equal number of Ti^{4+} to Ti^{3+}. In layer 3 and beyond, reduction will result in the formation of O^{2-} bulk vacancies. In this case each vacancy requires the reduction of two Ti^{4+} to Ti^{3+} ions.

In summary the formation of a surface vacancy pair in layer 1 requires no reduction; the formation of a shallow well of four vacancies in layers 1 and 2 requires the reduction of two Ti^{4+}; while the formation of a six-vacancy well in layers 1, 2, and 3, requires only the reduction of six Ti^{4+} ions.

It is important to note that vacancies need not always be in the immediate vicinity of the reduced titanium ions. They move about at high temperatures and may form transient pairs, strands, clusters, or other configurations. For example, a diffusion path along the ⟨001⟩ axis of rutile may form as shown in Fig. 3b (identical to Fig. 3a except that four O^{2-} have been omitted). The most restrictive dimension within this path or cluster is about 3.1 Å, which is the opening between adjacent titanium ions along the ⟨100⟩ or ⟨010⟩ axis. The cluster is appreciably wider in other directions and may reach dimensions greater than 4 Å. As such, it can hold at the same time metal atoms and one small molecule, such as H_2, O_2, H_2O, CO, CH_4.

The other two polymorphs of TiO_2 (anatase and brookite) exhibit more open cation sublattices than rutile in some directions (*18*), and as such should not hinder oxygen diffusion in those directions. Finally, partial reduction of rutile yields a series of titanium suboxides known as the Magneli phases or "shear structures" whose composition is given by

$$Ti_nO_{2n-1},$$

where $10 \geq n \geq 4$. Their structures follow the general geometric principles of homologous series derived by Magneli in 1948 for molybdenum oxides (*25*) and later extended to oxides of (Mo–W), V, Ti, (Ti–Cr), and (Ti–Nb) by various workers (*26*). In the case of titanium suboxides the shear structures consist of slabs of rutile of infinite extension in two dimensions and of a characteristic finite thickness in a third direction (*26*). Schematic representations of rutile and two shear phases are shown in Fig. 5. Within the slabs, diffusion should take place as in rutile. The shear phases, as well as TiO_2, are capable of exhibiting oxygen vacancies.

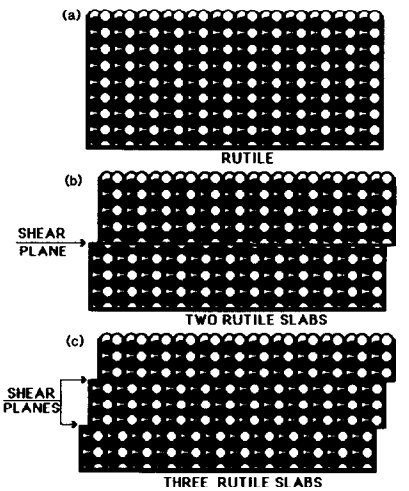

FIG. 5. Schematic representation of the rutile structure viewed in the ⟨100⟩ or ⟨010⟩ direction and of two shear structures consisting of rutile slabs of infinite dimensions in two directions and of finite thickness in the other. The thickness is determined by the composition: Ti_nO_{2n-1} for $10 \geq n \geq 4$. As n decreases (with reduction), the thickness decreases.

The Metals

The metals selected to illustrate our model are Rh, Pd, Pt, and Ir. They are among the most widely studied elements in SMSI and the first three were part of the original work of (*1*). They do not react with the oxide supports typically encountered in SMSI and their oxides are readily reduced in H_2. Furthermore they all possess atomic radii very close to that of O^{2-} and therefore can tightly fit in a vacancy. We have also considered base metals such as Fe, which has been studied by Tatarchuk *et al.* (*27–29*), and Ni, a much studied element in SMSI. However, since these metals are likely to react under HTO to form compounds (Fe_2TiO_5, etc.) and are much smaller in size than O^{2-}, they will be mentioned only briefly in this paper. Under LTR and HTR they exhibit SMSI properties and in fluorite-type supports, their small size makes diffusion into the bulk easier than for Group VIII noble metals.

Rh, Pd, Ir, and Pt have the fcc structure O_{h-5} (Fm3m-type A1) (*22*). A simple relationship allows the calculation of their radius r_A from the unit cell edge a_0:

$$r_A = \frac{a_0}{\sqrt{8}}. \qquad (2)$$

Table 3 gives the unit cell edge and the calculated radii of the metals. Note the closeness of these atomic radii with the values for O^{2-} shown in Tables 1 and 2.

TABLE 3

The Noble Metals

Metal	Unit cell edge[a] (Å)	Atomic radius (Å)
Rh	3.804	1.345
Ir	3.839	1.357
Pd	3.890	1.375
Pt	3.924	1.387

[a] From (*22*).

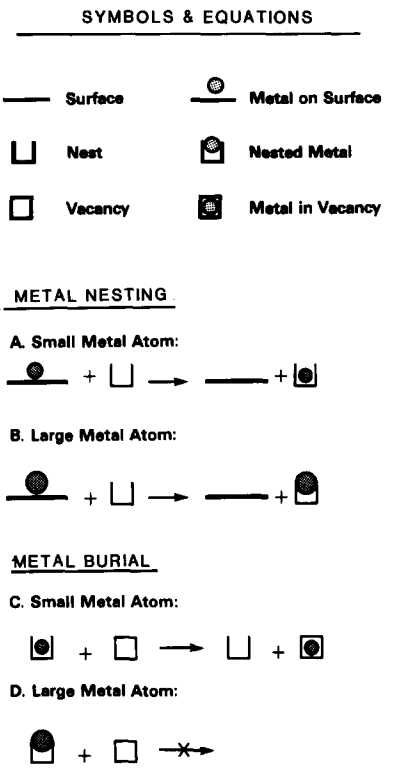

FIG. 6. Symbolic equations of the nesting transition for a small metal atom (A) and a large metal atom (B). There are no barriers to the transition surface to nest. Metal burial may occur for relatively small metals (C) but should not occur for metals which are much larger than the vacancy (D).

THE VACANCY INTERACTION MODEL

We propose a generalized model in which strong metal–support interactions result from the occupancy of individual vacancies or nests as well as clusters or wells, by metal atoms (see Fig. 6 for symbols and equations). The sections which follow discuss, in specific terms, at the atomic level, the operative mechanisms for the various interaction phenomena involving vacancies.

Surface Nesting

Nests are relatively easy to form by dehydration of hydroxylated surfaces or by chemical reduction of reducible oxides. Noble metal atoms located on an ideal support surface (Fig. 1b) will exhibit a weak

physical interaction with said surface. In such cases the atoms will migrate, at high temperatures, until they meet and coalesce to form large crystallites which results in loss of metal surface area, a decrease in sorptive capacity, and a decrease in catalytic activity. The driving force for the formation and growth of crystallites is the high surface tension which Rh, Pd, Ir, and Pt possess (1.47 to 2.25 N · m^{-1} at their melting points) (*24*) which correspond to surface energies in the range of 14 to 23. At lower temperatures they become appreciably higher.

On surfaces which possess nests, for example partially reduced CeO_2 or yttria doped thoria (Fig. 7a), the noble metals will also migrate over the ideal regions of the surface. However, when they meet nests, the atoms may drop into the surface defects (Fig. 7b). We call this phenomenon metal "nesting" and we consider nested atoms to be always more stable than the corresponding atoms on ideal surfaces. Figure 7c is a graphic, qualitative representation of the physical interaction energy (E) of a Pt atom with reduced ceria as a function of the distance (z) from the center of the nest. The Pt atom coordinates are (0, 0, z) and those of the nest (0, 0, 0). Note that in the graph $E(z)$ decreases as the metal approaches the support surface, reaches a minimum at a point N well into the OH^- layer and very rapidly swings upward as the metal is blocked from further penetration by the strong repulsive forces from the crystal lattice ions. This plot is not unlike that for $E(z)$ vs z for Pt on an ideal surface, in which case the minimum is shallow and located further out. Large atoms do not penetrate as much into the nest as small ones. For a given distance (z), the value of $E(z)$ is determined by the relative values of the forces involved. In general at distances greater than about two O^{2-} radii, the dominant force between the crystal and the metal atom, which is of the London type, is attractive and the resulting interaction energy is proportional to z^{-3} (*30, 31*), while at very short distances the dominant force is highly repulsive.

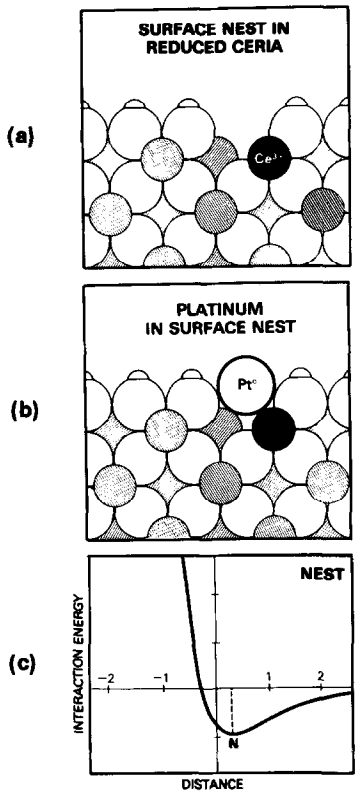

FIG. 7. (a) Cross section of CeO_2 showing the substitution of a Ce^{4+} by Ce^{3+} and the elimination of one OH^- from the surface, forming a nest (N). (b) Same as (a) with the surface nest occupied by a Pt^0 atom. (c) Qualitative plot of the physical interaction energy between Pt^0 and a nest on CeO_2 as a function of the distance from the center of the nest (measured in oxygen ionic radii).

Since for any of the defect fluorite-type supports, vacancies exist in the bulk and on the surface (nests) and freely move about at high temperatures, an equilibrium should be established between vacancies and nests, as shown by symbolic Eq. (3):

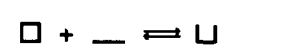
(3)

We have stated that the nesting transition energies (ΔE) of the reactions shown in Figs. 6a and 6b are always favorable regardless of the metal size. This may be represented by Eq. (4):

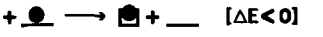

(4)

Combining Eqs. (3) and (4) gives Eq. (5):

(5)

which implies that the transition energy associated with the nesting reaction in any oxide support should favor migration of bulk vacancies to the surface to become metal-occupied nests.

According to the vacancy model, nesting is not limited to single, isolated atoms. It can also take place with atoms which are part of metal crystallites. This may happen when vacancies, driven by the nesting interaction energy, migrate to the metal–support interface and become occupied by metal atoms. For high values of ΔE, the interaction is strong enough to anchor the crystallites to the support, cause them to spread, and prevent their migration and sintering. This type of interaction may occur with reducible supports, as well as with "doped," nonreducible oxides. In some instances it may happen through surface dehydroxylation. In all cases, although to different degrees, it leads to improved metal dispersion and stability, which in turn mean high sorption and high catalytic activity and stability.

The value of ΔE depends on the relative size of the metal atom, the nature of the oxide support, the arrangement of the ions around the metal, and the electronic structure of the neutral metal atom.

Surface nesting is likely to occur to some degree in most oxide phases at high temperature because of the formation of nests through surface dehydration; however, the nesting energy may not always be significant in relation to other factors, for example, metal surface energy, compound formation, impurity effects. In general we envision strong metal–support interaction when the size of the metal is close to that of the nest. In such cases the metal can penetrate deep into the hydroxylated surface layer and become highly coordinated and strongly attached. In contrast when the metal atom is much larger than the nest, it cannot fully penetrate which prevents very strong interaction. Finally, when the metal atom is appreciably smaller than the nest, penetration should be easy, but symmetrical coordination would be unlikely. In spite of this the interaction might still be very strong since under these conditions the metal atom may reach reduced lattice cations, which may cause a degree of charge transfer. At this point the interaction will no longer be solely physical in nature and its value may increase markedly. In this specific aspect and in a qualitative sense only, we concur with Horsley's model II (*7*), but we do not attribute the loss of sorptive and catalytic properties to the charge transfer. In contrast, our model assumes that for relative small charge transfers, the nested metal atoms virtually retain their basic properties and therefore exhibit "normal" sorptive and catalytic properties.

In contrast to other SMSI models, the vacancy model accounts for catalytic and sorptive losses through metal burial, as will be discussed next.

Bulk Penetration

Besides surface nesting, our model proposes a mechanism for nested metal atoms to penetrate into the crystal structure of the oxide support, provided that vacancies exist or are created next to the metal. Two configurations are visualized. In one the metal atom penetrates into the bulk layers of the support but remains accessible to surrounding gases. In the other the metal atom, after bulk penetration, is covered by O^{2-} (and/or OH^-) which migrate over the crystal surface. The metal becomes isolated and cannot interact with the surrounding gases. The metal atom is *buried.*

Figures 8a and 8b illustrate the penetration of a Rh atom in a fluorite-type structure (nest to vacancy transition), while Fig. 8c is a qualitative representation of the metal support interaction energy (E) as a function of distance (z), for a system which exhibits a nest and an adjacent vacancy. The right side of the curve, for $z > 0$, which includes the stable nested configuration (N), is es-

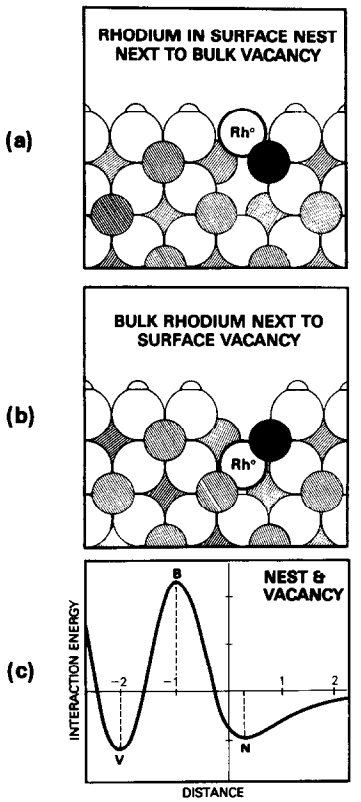

FIG. 8. (a) Same as Fig. 7b showing a vacancy below the nest which is occupied by Rh^0. (b) Same as 8a after the Rh^0 has diffused into the vacancy in the first bulk layer. The cations between the nest and vacancy constitute a diffusion barrier (B) for the burial transition nest (N) to vacancy (V). (c) Qualitative plot of the physical interaction energy between Rh^0 and a nest and an adjacent vacancy set, in CeO_2, as a function of the distance from the center of the nest (measured in oxygen ionic radii).

sentially the same as that shown in Fig. 7c. However, for $z < 0$ the shape of the curve reflects the presence of the vacancy below the nest. The repulsive forces are mainly due to the two cations which laterally block penetration, but do not include the frontal blocking of the missing O^{2-}. As such, the $E(z)$ maximum is reached at the narrowest point B in the diffusion path, located at $z = -1$. Beyond B, the absence of O^{2-} allows for easy penetration and the curve sharply turns downward and reaches a minimum at point V, which corresponds to the center of the vacancy at $z = -2$. Beyond V the curve becomes very similar to the ascending branch shown in Fig. 7c. The relative positions of points N, B, and V, will depend on the specific metal–support system under consideration.

Three major factors determine the likelihood of penetration. The first is the size of the metal in relation to the vacancy. The second is the energy of the system for the buried condition in relation to that for the nested condition (points N and V of Fig. 8c) and the third is the activation enthalpy of the transition N to V represented by the barrier N to B in Fig. 8c.

As already discussed, we believe that the interaction energy of a metal in a nest will always be more favorable than on an ideal surface regardless of size considerations and degree of nesting. The situation is quite different for the buried condition. To begin with, if the metal atom is much larger than the vacancy the interaction energy will not be favorable, which would negate stable burial. Even if the burial energy were not adverse, the transition would only be favored if burial were more stable than nesting. Equations C and D of Fig. 6 symbolically represent the burial phenomena for different sizes.

Finally, even with favorable energy terms for burial, the N to V transition will not occur to any significant degree at low temperatures if the activation enthalpy is high. We have shown that the activation enthalpy for O^{2-} diffusion in fluorite-type oxides is quite high because of the compact arrangement of the cations. The most restrictive opening in their diffusion path is about 68% of their size and since the sizes of Rh, Pd, Ir, and Pt are nearly equal to those of O^{2-}, one may infer that diffusion of these metals should also be hindered by the cation sublattices.

For reducible oxides with "open" regions of cations and "compact" regions of O^{2-}, diffusion should be easier. For example, in cassiterite-type oxides, which have O^{2-} doublets in every [001] layer, selective elimination of OH^- or O^{2-}, by dehydration

or reduction, could create, in principle, large diffusion paths with no barriers nor obstacles to overcome (Figs. 3b and 4). However, the likelihood of formation of long, empty channels must be considered low. Our model does not rely on their formation, followed by diffusion of the noble metals into them, although their existence is not negated and would not be in conflict with the model. Instead, we favor a mechanism which simultaneously allows support reduction, vacancy formation, and metal penetration. The proposed mechanism, proceeds along these lines:

1. The metal is deposited onto the support in a highly dispersed condition.
2. The system in the presence of H_2, at high temperature, causes H_2 dissociation and spillover (*32*).
3. The atomic H readily diffuses into the support and reduces nearby cations, creating nests and vacancies and forming water which diffuses out.
4. The metal atoms occupy the nests and vacancies, thereby beginning the penetration process.
5. H_2 adsorption, dissociation, and spillover continue, causing additional reduction and formation of more vacancies in the vicinity of the metal. Further penetration follows. According to our view the metal–H sets become chemical "drills" in the crystal directions which simultaneously allow metal and H_2 diffusion (in) and water diffusion (out).
6. In reducible oxide supports with the cassiterite structure (as well as other supports with open cation sublattices), the penetration can proceed to appreciable depths at the temperatures involved in SMSI.
7. Following penetration, the metal atoms which remain accessible to surrounding gases will show sorptive and catalytic properties. However, when essentially all the metal has diffused into the support, the fraction of accessible atoms will be small and the sorptive and catalytic properties will be affected accordingly.
8. Furthermore surface migration of O^{2-} and/or OH^- can cover the metal clusters or strands bringing about burial and complete elimination of sorptive and catalytic properties.
9. Finally during HTO with H_2O or O_2, the lattice will be restored to its full complement of O^{2-} by gradually filling the vacancies and driving the metal back to the surface. (Atomic oxygen may also be involved in the oxidation step).

These phenomena can take place with single metal atoms but are more likely to occur with small metal crystallites.

Similar diffusion and burial should also be possible in the other two-TiO_2 polymorphs since the Ti^{4+} sublattices are more open than in rutile. Diffusion could also be possible to some extent in the shear phases, since they consist of slabs with the rutile structure.

In general, diffusion into the bulk should be possible for the following:

(1) Ionic, reducible oxides with "open" regions of cations and "compact" regions of O^{2-} such as, for example, some of the V, Mn, Nb and Ta oxides, which have also been shown to exhibit SMSI.

(2) Also, to some extent, for nonreducible oxides which exhibit a high concentration of vacancies, through isomorphous replacement of cations, and more likely for solid solutions of reducible with nonreducible but doped oxide phases.

(3) Also, although not as likely, for ionic oxides of very high surface area capable of reaching high concentrations of nests through dehydration at high temperatures.

Combinations of 1, 2, and 3 above should work to varying degrees.

Figure 9 illustrates several configurations of the Pt–TiO_2 system at various stages of the SMSI process. All sketches represent an equal number of Pt and Ti atoms. However, they differ in the number of O^{2-}, depending on the degree of reduction of the support. Sketch (a) represents rutile with a

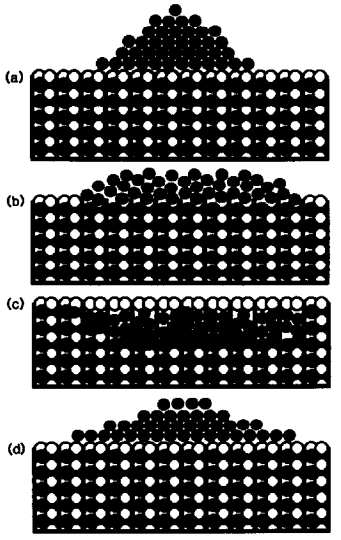

FIG. 9. Representation of SMSI stages for platinum on rutile. (a) Small Pt crystallite on surface. (b) Partly reduced surface with nests and spread Pt. (c) Buried Pt showing pseudomorphism (pillbox). (d) Oxidized system. Pt driven back to surface.

small, globular Pt crystallite on its surface. The rutile has not been reduced and a full complement of O^{2-} is shown. Sketch (b) illustrates the start of support reduction. Surface vacancies have been formed and occupied by Pt, causing the metal particle to spread and become thinner. Sketch (c) shows clusters and strands of metal atoms which have diffused into the support structure following further O^{2-} removal during reduction while the metal is covered by surface O^{2-} (or OH^-). Finally structure (d), following HTO, is essentially equal to the one shown in (a). The support has been restored to a full complement of O^{2-} and the metal has been driven back to the surface where its catalytic and sorptive properties can again be manifested.

An important feature of our model is the fact that the metal atoms, upon penetration, will occupy the sites of the O^{2-} in the lattice or in some manner relate to their positions. The net result should be a degree of regularity and symmetry determined, in part, by the nature of the O^{2-} sublattice, through pseudomorphism.

GENERAL DISCUSSION AND OVERVIEW

This section deals primarily with a comparison of our vacancy model with the support migration (M) model, which is currently the most widely accepted explanation and rationalization of SMSI. Other important aspects of the V model are also discussed.

Within the SMSI field, the single most important feature shared by the V and M models is the nature of the surface following HTR. Both models agree that the resulting surfaces comprise reduced support cations and suboxides and that virtually all the metal is blocked by an oxide outer layer. Both models also offer parallel explanations for the reversibility observed after HTO followed by LTR. In essence, the two models account for the resulting properties of the reduced system in terms of virtually the same final configurations. Furthermore, both models can account for activity decreases with progressively longer HTR and show the square-root dependence on time expected for diffusion processes.

It, therefore, appears to matter little whether the support migrated through or over the metal to cover and mask it, or the metal migrated into the support to become covered and buried.

That being the case: Why the need for yet another SMSI model? From an overall point of view, we should state at the outset that the V model is not limited to SMSI and addresses several other phenomena. Furthermore, the V model has predictive value for strong metal–support interactions in general and SMSI in particular. Predictions may be made by applying relatively simple criteria, using well-established properties, facts, and processes to a candidate system. The information needed to evaluate a candidate includes detailed crystal structures, atomic and ionic sizes, reduction thermodynamics, introduction of dopants capable of isomorphous substitutions, etc. This predictive capability is not readily apparent in the M model as will be discussed later.

The V model's predictive nature lies in the fact that it is based on detailed accounts at the atomic level of the mechanisms involved in LTR, HTR, and HTO. Specifically we base our model on the *individual* migration of O^{2-} ions (O^{2-} vacancies), H, O, and metal atoms, and very small molecules such as H_2, O_2, and H_2O, all of which are well documented in the literature. Regarding SMSI, the key mechanism of the V model is the migration of the metal into the support and its subsequent burial by O^{2-} or OH^-. The metal migration depth, in this step, corresponds approximately to the thickness of the metal particles following HTR, which has been shown to be quite small (pillbox or raft morphology), and well within the migration ranges of Group VIII metals. The O^{2-} or OH^- migration distances required to effect metal coverage correspond to approximately the radius of the metal particles after HTR (of the order of 10 nm) (*13*), again well within the known ranges for such migrations on crystal surfaces at SMSI temperatures.

In its present form, it would be very difficult to make specific predictions using the M model. The main reason for this limitation lies in the fact that it does not provide criteria to define the support suboxide species which must migrate over the metal particle to cover it. For the best known SMSI support (TiO_2) some of the possible suboxides are TiO, Ti_2O_3, and Ti_3O_5, which are not obtained by reduction in H_2 under SMSI conditions, and Ti_4O_7, Ti_5O_9, Ti_6O_{11}, Ti_7O_{13} . . . , which are too large for migration over appreciable distances. Less is known for other supports, for example, the oxides of Ta, Nb, Mn, and V. Besides, since very little is known about the properties of the suboxides, such as surface and interfacial energies, and migration activation enthalpies, it is virtually impossible to decide a priori whether any given reducible oxide will or will not exhibit SMSI.

In general the M model appears to be mainly an account and rationalization of observed properties and phenomena, rather than a set of criteria capable of generalization and prediction. In order to illustrate the basic differences between the M and the V models we pose the following question: Why does the Pt–TiO_2 system show SMSI, while the Pt–CeO_2 system does not (*12*)?

Specifically, one may state that TiO_2 is reducible to Ti_2O_3 and CeO_2 to Ce_2O_3, that the free energies of reduction, per mole of H_2 consumed, at 773 K are +22.8 and +15.7 kcal, respectively; that the thermodynamics for reduction are favorable for both suboxides in a stream of H_2 with a P_{H_2O} to P_{H_2} ratio of less than 10^{-7}; that the activation enthalpies for reduction must block the reactions, since neither suboxide is formed in a stream of pure H_2 at 773 K; that little or no data are available on the surface energies of the various oxides; that the melting points indicate a more stable solid structure for CeO_2 (2873 K) than for TiO_2 (1913 K), a trend which is reversed for the suboxides (1965 K for Ce_2O_3 and 2403 K for Ti_2O_3); that at the melting points, both Ti oxides decompose to lower oxides while the Ce oxides remain unchanged; and finally that the crystal structures are profoundly different, as discussed in detail in the Introduction.

Given the M model, there seems to be no a priori reason to predict SMSI behavior for one dioxide over the other. However, within the V model, the nature of the crystalline structures indicates that the Pt atoms are too large to easily penetrate past the first cation layer in CeO_2, even following HTR and the creation of vacancies, while in TiO_2 the existence of an open cation sublattice makes possible, upon reduction and O^{2-} elimination, a diffusion path and therefore easy metal bulk penetration. Within the V model, the criteria for predicting strong surface metal–support interaction for CeO_2, and SMSI for TiO_2 are established.

The following are the basic premises and generic criteria for the vacancy, physical interaction model:

1. The support interacts with the metal through O^{2-} vacancies. The cation sublattice does not change, although some minor adjustments may occur as in the shear phases (*5, 25, 26*).

2. The vacancies result from dehydration, reduction, thermal dissociation, and isomorphous cation substitutions.

3. The concentration of vacancies relative to the metal determines the degree and also the kind of interaction:

a. Low concentration limits interaction to the surface.

b. High concentration allows bulk diffusion and burial.

4. The "potential" diffusion path into the support is set by the support crystal structure:

a. Open cation sublattices allow for easy diffusion.

b. Compact cation sublattices will block metal diffusion into the bulk creating high activation enthalpy.

5. Temperature in relation to activation enthalpy and vacancy concentration in relation to metal level determine metal partition (burial, surface rafts, small, well dispersed crystallites, or sintered large aggregates).

6. Virtually all hydroxylated metal oxide supports will show surface interaction at high temperature.

7. Virtually all supports with low levels of dopants capable of generating vacancies, even after HTO, will show surface interactions at all temperatures.

8. Virtually all supports with high levels of dopants, capable of creating high vacancy concentrations after HTO, should in principle be able to cause complete metal burial at sufficiently high temperatures.

9. The best candidate systems for SMSI are reducible oxide supports with open cation sublattices, which do not undergo phase transformation upon reduction, in conjunction with noble metals capable of H_2 dissociation and spillover.

10. Group VIII noble metals will show SMSI following HTR on supports with open cation sublattices and reversibility following HTO and LTR (*3, 4 ,6*).

11. Other Group VIII metals will show SMSI after HTR but may not show reversibility under HTO/LTR due to compound formation and changes in crystalline structures (*27–29*).

12. Other metals may also be involved in SMSI. Atomic size, oxide reducibility, and tendency to form compounds with the support are key factors. Easily reduced supports do not require atomic H. If H is needed it may be provided by a "promoting" metal such as in the Ag(Pt)–TiO_2 system (*33*).

In the previous sections we have reviewed and discussed the work and data of others, and relied to some extent on their findings to formulate our own views and model. It is therefore proper to attempt to relate their work to the proposed vacancy model, its evolution, and its formulation.

The idea of relating surface metal–support interactions to O^{2-} vacancies goes, at least, back to the work of (*1*), which appeared in 1974. The occupancy of surface O^{2-} vacancies by noble metal atoms was postulated to be the reason for a metal–support interaction capable of competing with metal sintering at high temperatures, under oxidation conditions.

In the second paper on SMSI in 1978, Tauster and Fung (*4*) speaking of the role of O^{2-} vacancies and associated reduced cations such as Ti^{3+}, state "the significance of oxygen anion removal . . . seems rather plausible . . . interaction with an *aggregate* of metal atoms requires a high local concentration of such cations [hence O^{2-} vacancies] and that reduction of the surface is required to bring this about." In 1979, Horsley (*7*) proposed model II, in which a Pt atom occupies an O^{2-} vacancy in the octahedral TiO_6^{8-} cluster. Both of these pioneer papers invoked the presence of O^{2-} surface vacancies in their explanation and modeling of SMSI. However, the thrust in these publications was to account for SMSI

through charge transfer from the reduced cation to the metal.

In 1979 Baker *et al.* (*5*) provided experimental data which supported the view of (*1*). Their papers reads, "the metal dispersion was significantly more stable on titanium oxide than [on] the other supports," which were nonreducible alumina, silica, and carbon, hence, with very few or no vacancies. On TiO_2 they observed thin, polygonal metal morphologies and coined the term "pillbox" which together with the term "raft" has become widely used in this field. This unusual morphology, not accounted for by the M model, can be explained through the V model on the basis of pseudomorphism.

The second paper by Baker *et al.* (*6*) in 1979 reads, "When Pt in the SMSI state was oxidized, there was an appreciable increase in the growth rate of the Pt particles, comparable to that found on conventional supports." These observations again agree with the V model, since upon oxidation the vacancies would disappear and the TiO_2 would become a "conventional support."

In both of these papers, Baker *et al.* (*5, 6*) also speak of the catalytic effect of Pt in the reduction of TiO_2 to Ti_4O_7 and clearly demonstrate the need for atomic H to effect deep reduction at the temperatures used. In a later publication (*33*) they extend the work to the Ag–TiO_2, and Ag(Pt)–TiO_2 systems and show the role of the promoting metal (Pt) in achieving pillbox morphology for the Ag, a metal which is not capable of H_2 dissociation. To their conclusions, we add our views: Thermodynamically, hydrogen reduction beyond Ti_4O_7 is possible. However, reduction creates shear phases which restrict O^{2-} and H_2O diffusion to varying degrees. Diffusion across the reduced rutile slabs is not affected; however, diffusion through the shear planes is difficult due to the high packing and closeness of the titanium ions at these interfaces. The resulting barriers and the compact nature of the cation sublattice in the next suboxide (Ti_3O_5), which is not a shear phase, makes reduction beyond Ti_4O_7 unlikely, and thus, this suboxide becomes the end member of the HTR series. We do not see Ti_4O_7 to be fundamentally related to SMSI, but visualize it as an incidental occurrence related to the activation enthalpy for O^{2-} and H_2O diffusion across the shear planes or within Ti_3O_5.

Finally, this overview should not be concluded without reference to the work of Tatarchuk and Dumesic (*27–29*) on Fe/TiO_2 model supported catalysts. They were the first authors in the SMSI field to recognize the possibility of metal diffusion *into* the support. In their last paper they conclude, "Indeed, the diffusion of iron into the support and the reduction of titania may well be interrelated. Specifically, iron facilitates the reduction of titania, and the removal of oxygen from titania during this reduction, allows iron to diffuse into the support." A statement which clearly anticipates some of our views. The lack of reversibility in their system is most likely due to free energy considerations for the reduction of $FeTi_2O_5$ or conversely the activation enthalpy associated with such reduction.

SUMMARY

A generalized model for strong metal–support interaction and for SMSI has been formulated and proposed which is based on the occupancy of oxygen ion vacancies by metal atoms. The model has predictive value. It highlights the nature of the cation sublattice in the oxide phases. Oxides with uniformly compact cation sublattices in which the opening between adjacent cations is always smaller than the metal atoms will block their diffusion at low and intermediate temperatures. Fluorite-type supports belong to this class of oxides. For such reducible supports, the model predicts easy surface removal of O^{2-} or OH^- and easy metal accessibility of the resulting nests. For nonreducible oxides, dehydration at high temperatures, or lower valence cation substitution provides the surface nests involved in the metal–support inter-

action. However, the presence of a high barrier for bulk diffusion makes burial difficult. In these types of supports the most favored metal configuration, upon creation of surface nests, appears to be small, thin, flat crystallites with many of the atoms nested in the support surface (pillbox or raft structures). This configuration takes into account the high surface energy of the metal, and the strong interaction energy of nesting.

In contrast, oxide phases in which the opening between adjacent lattice cations is large in relation to O^{2-}, at least in some crystallographic directions, exhibit easy oxygen diffusion and reduction. Such phases will also allow bulk diffusion of neutral metal atoms. Cassiterite-type oxides, such as rutile, fall in this class, as well as other metal oxides whose cation radius falls between about 0.5 and 0.75 Å. In general, any oxide phase which can be readily reduced in hydrogen at intermediate temperatures will likely exhibit an open cation sublattice in some crystallographic direction. Easy diffusion can lead to metal burial and the appearance of SMSI properties. Finally oxidation will fill the vacancies, drive the metal back to the surface, and restore catalytic, sorptive, and morphological properties after LTR.

ACKNOWLEDGMENTS

We thank R. G. Donnelly, J. E. Kubsh, N. R. Laine, and N. D. Spencer for many valuable discussions, suggestions, and advice. We also thank Professor R. S. Drago for his encouragement toward publication following the presentation of the subject at the Florida Conference on Catalysis in April 1985.

REFERENCES

1. Sanchez, M. G., Maselli, J. M., and Graham, J. R., U.S. Pat. 3,830,756, August 20, 1974.
2. Sergeys, F. J., Maselli, J. M., and Ernest, M. V., U.S. Pat. 3,903,020, Sept. 2, 1975.
3. Tauster, S. J., Fung, S. C., and Garten, R. L., *Amer. Chem. Soc.* **100,** 170 (1978).
4. Tauster, S. J., and Fung, S. C., *J. Catal.* **55,** 29 (1978).
5. Baker, R. T. K., Prestridge, E. B., and Garten, R. L., *J. Catal.* **56,** 390 (1979).
6. Baker, R. T. K., Prestridge, E. B., and Garten, R. L., *J. Catal.* **59,** 293 (1979).
7. Horsley, J. A., *J. Amer. Chem. Soc.* **101,** 2870 (1979).
8. Huizinga, T., and Prins, R., *Stud. Surf. Sci. Catal.* **11,** 11 (1982).
9. Huizinga, T., van't Blik, H. F. J., Vis, J. C., and Prins, R., *Surf. Sci.* **135,** 580 (1983).
10. Huizinga, T., and Prins, R., *J. Phys. Chem.* **87**(1), 173 (1983).
11. Short, D. R., Mansour, A. N., Cook, J. W., Jr., Sayers, D. E., and Katzer, J. R., *J. Catal.* **82,** 299 (1983).
12. Meriaudeau, P., Dutel, J. F., Dufaux, M., and Naccache, C., *Stud. Surf. Sci. Catal.* **11,** 95 (1982).
13. Santos, J., Phillips, J., and Dumesic, J. A., *J. Catal.* **81,** 147 (1983).
14. Resasco, D. E., and Haller, G. L., *J. Catal.* **82,** 279 (1983).
15. Horsley, J. A., *J. Catal.* **88,** 249 (1984).
16. Vannice, M. A., and Sudhakar, C., *J. Phys. Chem.* **88,** 2429 (1984).
17. DeCanio, S. J., Apple, T. M., and Dybowski, C. R., *J. Phys. Chem.* **87,** 194 (1983).
18. Wyckoff, R. W. G., "Crystal Structures," 2nd ed., Vol. 1. Wiley, New York, 1963.
19. Etsell, T. H., and Flengas, S. N., *Chem. Rev.* **70**(3) (1970).
20. Freer, R., *J. Mater. Sci.* **15,** 803 (1980).
21. Murch, G. E., and Nowick, A. S., Eds., "Diffusion in Crystalline Solids," Chap. 3, Academic Press, Orlando, FL, 1984.
22. Donnay, J. D. H., and Donnay, G., Eds., "Crystal Data: Determinative Tables," 2nd ed. Amer. Crystallographic Assoc., 1963. Washington D.C.
23. Dana, J. D., and Dana, E. S., "The System of Mineralogy," 7th ed. Vol. 1, p. 611. Wiley, New York, 1955.
24. "Handbook of Chemistry and Physics," 65th ed. CRC Press, Cleveland, OH, 1984.
25. Magneli, A., *Acta Chem. Scand.* **2,** 501 (1948).
26. Andersson, S., and Jahnberg, L., *Arkiv Kemi* **21,** 413 (1963).
27. Tatarchuk, B. J., and Dumesic, J. A., *J. Catal.* **70,** 308 (1981).
28. Tatarchuk, B. J., and Dumesic, J. A., *J. Catal.* **70,** 323 (1981).
29. Tatarchuk, B. J., and Dumesic, J. A., *J. Catal.* **70,** 335 (1981).
30. Lennard-Jones, J. E., and Dent, B. M., *Trans. Faraday Soc.* **24,** 92 (1928).
31. Clark, A., "The Theory of Adsorption and Catalysis." Academic Press, New York, 1970.
32. Boudart, M., and Djéga-Mariadassou, G., "Kinetics of Heterogeneous Catalytic Reactions." Princeton Univ. Press, Princeton, NJ, 1984.
33. Baker, R. T. K., Prestridge, E. B., and Murrell, L. L., *J. Catal.* **79,** 348 (1983).